

Robust Fault Detection and Reconfiguration in Sampled-Data Uncertain Distributed Processes

Zhiyuan Yao and Nael H. El-Farra[†]

Department of Chemical Engineering & Materials Science
University of California, Davis, CA 95616 USA

Abstract—This paper focuses on robust model-based fault detection and fault-tolerant control of spatially distributed processes described by parabolic partial differential equations (PDEs) subject to time-varying external disturbances, control actuator faults and measurement sampling rate constraints. Using an approximate finite-dimensional system that captures the dominant dynamics of the PDE, an observer-based output feedback controller is initially designed to enforce robust stability with an arbitrarily small ultimate bound on the closed-loop state in the absence of faults. A finite-dimensional inter-sample model predictor is then embedded within the controller to provide the observer with estimates of the measured output between the sampling times, and the state of the model is updated using the measured output at each sampling time. By formulating the sampled-data finite-dimensional closed-loop system as a combined discrete-continuous system, a necessary and sufficient condition for robust closed-loop stability is obtained and used to explicitly characterize the tradeoffs between the sampling rate, the degree of model uncertainty, the disturbance size, the size of the achievable ultimate bound on the closed-loop state, and the choice of actuator/sensor locations. Based on this analysis, a time-varying alarm threshold on the fault detection residual is obtained, together with an actuator reconfiguration law that determines the set of feasible fall-back actuators that preserve robust closed-loop stability. Finally, the result is illustrated through an application to a representative diffusion-reaction process.

I. INTRODUCTION

The growing emphasis on safety and reliability in industrial process operation over the past few decades have drawn increasing attention to the need for systematic methods for the detection and handling of faults. The realization that malfunctions in the control actuators, measurement sensors and process equipment, if not properly accounted for, can lead to substantial performance deterioration and even instability has motivated significant research work on the problems of fault detection and fault-tolerant control in both the industrial and academic communities (e.g., see [1]–[11] and the references therein). At this stage, however, only a few studies have been dedicated to the development of systematic methods for the diagnosis and handling of faults in spatially distributed processes. This is an important problem given that many industrial processes are characterized by spatial variations owing to the underlying physical phenomena such as diffusion, convection, and phase-dispersion, and are naturally

modeled by Partial Differential Equations (PDEs) (e.g., see [12]–[17] and the references therein). Examples of existing results for distributed parameter systems include methods for fault detection and accommodation using approximate finite-dimensional models (e.g., [18]–[20]), integrated fault diagnosis and reconfiguration-based fault-tolerant control of nonlinear distributed processes [21], [22], and safe-parking of transport-reaction processes [23].

Recently we developed in [24] a model-based approach for the detection and compensation of actuator faults in distributed processes described by parabolic PDEs with measurement sampling rate constraints. A key idea was to embed within the fault-tolerant control system an approximate model of the dominant process dynamic modes to provide the controller and fault detection filter with estimates of the measured output between sampling times, and to update the model state using the measurements whenever they become available from the sensors at discrete sampling times. An explicit characterization of the minimum allowable sampling rate was obtained leading to the derivation of explicit rules for fault detection and actuator reconfiguration.

In addition to handling sampling rate constraints, an important property that any model-based fault-tolerant control system must possess, in order to be well suited for practical implementation, is robustness with respect to uncertainties, such as time-varying exogenous disturbances, which are commonly encountered in process operation. External disturbances, if not properly accounted for in the fault-tolerant control system design, may not only degrade the stability and performance properties of the feedback controller, but can also erode the fault detection and control system reconfiguration capabilities, leading to false alarms and poor supervisory control.

Motivated by these considerations, we present in this work a robust fault detection and fault-tolerant control structure for sampled-data spatially distributed processes subject to time-varying external disturbances. The structure consists of a family of robust output feedback controllers that enforce robust closed-loop stability with an arbitrary degree of disturbance attenuation, observer-based fault detection filters that account for the discrete sampling of measurements and the disturbances, and a switching law that orchestrates the transition from the faulty actuator configuration to a healthy fall-back following fault detection. The rest of the paper is organized as follows. Following some preliminaries

[†] To whom correspondence should be addressed; E-mail: nheffarra@ucdavis.edu. Financial support by NSF CAREER Award, CBET-0747954, is gratefully acknowledged.

in Section II, an approximate finite-dimensional system is obtained using modal decomposition techniques, and used in Section III to design model-based output feedback controllers that robustly stabilized the closed-loop system in the absence of faults. An explicit characterization of the interdependence between the achievable ultimate bound, the sampling rate, the disturbance size, the plant-model mismatch, the spatial placement of the control actuator locations, and the controller/observer design parameters is obtained and used in Section IV to derive appropriate rules for robust fault detection and actuator reconfiguration based on the approximate finite-dimensional system. Finally, in Section V the proposed methodology is applied to achieve fault-tolerant stabilization of an unstable steady-state of a representative diffusion-reaction process under actuator faults and disturbances.

II. PRELIMINARIES

As a motivating example, we consider spatially distributed processes modeled by parabolic PDEs of the form:

$$\frac{\partial \bar{x}}{\partial t} = \alpha \frac{\partial^2 \bar{x}}{\partial z^2} + \beta \bar{x} + \omega \sum_{i=1}^m b_i^k(z) [u_i^k(t) + f_{ai}^k(t)] + v \sum_{j=1}^n d_j(z) \theta_j(t), \quad |\theta_j(t)| \leq \theta_b^j \quad (1)$$

$$k \in \mathcal{K} := \{1, 2, \dots, N\}, \quad N < \infty$$

$$y_l = \int_0^\pi q_l(z) \bar{x}(z, t) dz, \quad l = 1, \dots, p$$

subject to the boundary and initial conditions:

$$\bar{x}(0, t) = \bar{x}(\pi, t) = 0, \quad \bar{x}(z, 0) = \bar{x}_0(z) \quad (2)$$

where $\bar{x}(z, t) \in \mathbb{R}$ denotes the process state variable, $z \in [0, \pi]$ is the spatial coordinate, $t \in [0, \infty)$ is time, u_i^k denotes the i -th manipulated input associated with the k -th actuator configuration, $b_i^k(\cdot)$ is the actuator distribution function, f_{ai}^k denotes a fault in the i -th actuator of the k -th configuration, θ_j is an uncertain variable that represents an exogenous disturbance, θ_b^j is a positive real number that captures the maximum size of θ_j , $d_j(\cdot)$ is a square-integrable function that specifies the positions of action of the disturbance θ_j in the spatial domain, $y_l(t) \in \mathbb{R}$ is a measured output, $q_l(\cdot)$ is the sensor distribution function, the parameters $\alpha > 0, \beta, \omega, v$ are constants, and $\bar{x}_0(z)$ is a smooth function of z . Throughout the paper, the norm notations $|\cdot|, \|\cdot\|$ and $\|\cdot\|_2$ will be used to denote the standard Euclidean norm, the L_2 norm associated with a finite-dimensional Hilbert space, and the L_2 norm associated with an infinite-dimensional Hilbert space, respectively. Furthermore, a bounded linear operator \mathcal{N} is said to be power-stable if there exists positive real numbers β and γ such that $\|\mathcal{N}^j\| \leq \beta e^{-\gamma j}$, for any non-negative integer j . The spectral radius of a bounded linear operator \mathcal{N} is defined as $r(\mathcal{N}) = \lim_{j \rightarrow \infty} \|\mathcal{N}^j\|^{1/j} \leq \|\mathcal{N}\|$. From these definitions, it can be verified that \mathcal{N} is power-stable if and only if $r(\mathcal{N}) < 1$. Finally, the notation $x(t_k^-)$ will be used to denote the limit $\lim_{t \rightarrow t_k^-} x(t)$.

Using standard techniques from operator theory [25], the PDE of (1)-(2) can be formulated as an infinite-dimensional system of the following form:

$$\dot{x}(t) = \mathcal{A}x(t) + \mathcal{B}^k[u^k(t) + f_a^k(t)] + \mathcal{W}\theta(t), \quad x(0) = x_0 \quad (3)$$

$$y(t) = \mathcal{Q}x(t) \quad (4)$$

where $x(t) = \bar{x}(z, t)$, $t > 0$, $0 < z < \pi$, is the state function defined on the Hilbert space $\mathcal{H} = L_2(0, \pi)$ endowed with inner product and norm:

$$\langle \omega_1, \omega_2 \rangle = \int_0^\pi \omega_1(z) \omega_2(z) dz, \quad \|\omega_1\|_2 = \langle \omega_1, \omega_1 \rangle^{\frac{1}{2}} \quad (5)$$

where ω_1, ω_2 are two elements of $L_2(0, \pi)$, \mathcal{A} is the differential operator defined by $\mathcal{A}\phi = \alpha \frac{d^2 \phi}{dz^2} + \beta \phi$, $0 < z < \pi$, where $\phi(\cdot)$ is a smooth function on $(0, \pi)$ with $\phi(0) = \phi(\pi) = 0$, \mathcal{B}^k is the input operator defined by $\mathcal{B}^k u^k = \omega \sum_{i=1}^m b_i^k(\cdot) u_i^k$, $u^k = [u_1^k \ u_2^k \ \dots \ u_m^k]^T$, $f_a^k = [f_{a1}^k \ f_{a2}^k \ \dots \ f_{am}^k]^T$, \mathcal{W} is the uncertainty operator defined by $\mathcal{W}\theta = v \sum_{j=1}^n d_j(z) \theta_j(t)$, $\theta = [\theta_1 \ \theta_2 \ \dots \ \theta_n]^T$, \mathcal{Q} is the measurement operator defined by $\mathcal{Q}x = [\langle q_1, x \rangle, \langle q_2, x \rangle, \dots, \langle q_p, x \rangle]^T$, $y = [y_1 \ y_2 \ \dots \ y_l]^T$ and $x_0 = \bar{x}_0(z)$.

For \mathcal{A} , the eigenvalue problem is given by $\mathcal{A}\phi_j = \lambda_j \phi_j$, $j = 1, \dots, \infty$, where λ_j denotes an eigenvalue and ϕ_j denotes an eigenfunction. The solution to this eigenvalue problem is given by $\lambda_j = \beta - \alpha j^2$, $\phi_j(z) = \sqrt{\frac{2}{\pi}} \sin(jz)$, $j = 1, \dots, \infty$. By analyzing this solution, it can be seen that all the eigenvalues of \mathcal{A} are real and ordered. Also, for a given α , only a finite number of unstable eigenvalues exists, and the distance between two consecutive eigenvalues (i.e., λ_j and λ_{j+1}) increases as j increases. Furthermore, the spectrum of \mathcal{A} can be partitioned as $\sigma(\mathcal{A}) = \sigma_1(\mathcal{A}) \cup \sigma_2(\mathcal{A})$, where $\sigma_1(\mathcal{A}) = \{\lambda_1, \dots, \lambda_m\}$ contains the first m (with m finite) "slow" eigenvalues and $\sigma_2(\mathcal{A}) = \{\lambda_{m+1}, \lambda_{m+2}, \dots\}$ contains the remaining "fast" stable eigenvalues where $|\lambda_m|/|\lambda_{m+1}| = O(\epsilon)$ and $\epsilon < 1$ is a small positive number that characterizes the extent of separation between the slow and fast eigenvalues of \mathcal{A} . This separation property implies that the dominant dynamics of the PDE can be described by a finite-dimensional system, and motivates the application of modal decomposition techniques to decompose the infinite-dimensional system of (3)-(4) into the following form:

$$\dot{x}_s = \mathcal{A}_s x_s + \mathcal{B}_s^k [u^k + f_a^k] + \mathcal{W}_s \theta, \quad x_s(0) = \mathcal{P}_s x_0 \quad (6)$$

$$\dot{x}_f = \mathcal{A}_f x_f + \mathcal{B}_f^k [u^k + f_a^k] + \mathcal{W}_f \theta, \quad x_f(0) = \mathcal{P}_f x_0 \quad (7)$$

$$y = \mathcal{Q}_s x_s + \mathcal{Q}_f x_f \quad (8)$$

where $x_s = \mathcal{P}_s x \in \mathcal{H}_s := \text{span}\{\phi_1, \dots, \phi_m\}$ is the state of a finite-dimensional system that describes the evolution of the slow modes, $x_f = \mathcal{P}_f x \in \mathcal{H}_f := \text{span}\{\phi_{m+1}, \phi_{m+2}, \dots\}$ is the state of an infinite-dimensional system that captures the evolution of the fast eigenvalues, $\mathcal{H}_s, \mathcal{H}_f$ are modal subspaces of \mathcal{A} , and \mathcal{P}_s and \mathcal{P}_f are the orthogonal projection operators, where $\mathcal{A}_s = \mathcal{P}_s \mathcal{A}$ is an $m \times m$ diagonal matrix of the form $\mathcal{A}_s = \text{diag}\{\lambda_1, \dots, \lambda_m\}$, $\mathcal{B}_s^k = \mathcal{P}_s \mathcal{B}^k$ and $\mathcal{W}_s = \mathcal{P}_s \mathcal{W}$, $\mathcal{A}_f = \mathcal{P}_f \mathcal{A}$ is an unbounded differential operator which is exponentially stable (due to the fact that $\lambda_{m+1} < 0$ and the selection of \mathcal{H}_s and \mathcal{H}_f), $\mathcal{B}_f^k = \mathcal{P}_f \mathcal{B}^k$ and $\mathcal{W}_f = \mathcal{P}_f \mathcal{W}$. $\mathcal{Q}_s : \mathcal{H}_s \rightarrow \mathbb{R}^p$ and $\mathcal{Q}_f : \mathcal{H}_f \rightarrow \mathbb{R}^p$ are bounded operators associated, respectively, with the slow and fast parts of the measured output. Neglecting the fast and stable x_f -subsystem of (7), the following approximate, m -dimensional slow system can be obtained:

$$\dot{\hat{x}}_s = \mathcal{A}_s \hat{x}_s + \mathcal{B}_s^k [u^k + f_a^k] + \mathcal{W}_s \theta, \quad \bar{y} = \mathcal{Q}_s \hat{x}_s \quad (9)$$

where the bar symbol denotes that the variable is associated with a finite-dimensional system.

III. ROBUST STABILIZATION OF THE FAULT-FREE SAMPLED-DATA FINITE-DIMENSIONAL SYSTEM

A. Controller synthesis and implementation

Referring to the system of (9), we consider first the case when $f_a^k \equiv 0$, and synthesize, for each $k \in \mathcal{K}$, an observer-based output feedback controller of the form:

$$u^k(\bar{x}_s) = \mathcal{F}^k \eta, \quad \dot{\eta} = \widehat{\mathcal{A}}_s \eta + \widehat{\mathcal{B}}_s^k u^k + \mathcal{L}(\bar{y} - \mathcal{Q}_s \eta) \quad (10)$$

where \mathcal{F} is the feedback gain, η is an observer estimate of \bar{x}_s using \bar{y} , $\widehat{\mathcal{A}}_s$ and $\widehat{\mathcal{B}}_s^k$ are bounded operators that represent models of \mathcal{A}_s and \mathcal{B}_s^k , respectively, and \mathcal{L} is the observer gain. Note that in general $\widehat{\mathcal{A}}_s \neq \mathcal{A}_s$ and $\widehat{\mathcal{B}}_s^k \neq \mathcal{B}_s^k$ to account for possible plant-model mismatch. When the measured outputs are available continuously from the sensors, and in the case when $\widehat{\mathcal{A}}_s = \mathcal{A}_s$ and $\widehat{\mathcal{B}}_s = \mathcal{B}_s$, practical stability of the fault-free closed-loop system can be enforced by appropriate selection of the controller and observer gains. Specifically, it can be shown using standard Lyapunov arguments that given any set of positive real numbers, $\{\theta_b^1, \dots, \theta_b^n, r\}$, one can choose the controller and observer gains such that if $|\theta_i(t)| \leq \theta_b^i$ for all $t \geq 0$, the closed-loop states are ultimately bounded by r , where r can be chosen arbitrarily small by appropriate selection of \mathcal{F} and \mathcal{L} (i.e., by appropriate placements of the eigenvalues of $\mathcal{A}_s + \mathcal{B}_s^k \mathcal{F}^k$ and $\mathcal{A}_s - \mathcal{L} \mathcal{Q}_s$ in the left half of the complex plane).

Since the measured outputs are available from the sensors only at discrete time instances, however, the observer cannot be implemented directly. To deal with this problem, a model of the slow system of (9) is embedded within the controller to supply the observer with an estimate of the outputs between consecutive sampling times. The state of this inter-sample model predictor is then updated using the measured outputs whenever they become available from the sensors. This model-based control strategy is implemented as follows:

$$\begin{aligned} u^k(t) &= \mathcal{F}^k \eta(t), \quad t \in [t_j, t_{j+1}) \\ \dot{\omega}(t) &= \widehat{\mathcal{A}}_s \omega(t) + \widehat{\mathcal{B}}_s^k u^k(t), \quad \widehat{y}(t) = \mathcal{Q}_s \omega(t) \\ \dot{\eta}(t) &= \widehat{\mathcal{A}}_s \eta(t) + \widehat{\mathcal{B}}_s^k u^k(t) + \mathcal{L}(\widehat{y}(t) - \mathcal{Q}_s \eta(t)) \\ \widehat{y}(t_j) &= \bar{y}(t_j), \quad j \in \{0, 1, 2, \dots\} \end{aligned} \quad (11)$$

where ω is the model state (which is an estimate of \bar{x}_s), \widehat{y} is the model output (which is an estimate of \bar{y}), and $\Delta := t_{j+1} - t_j$ is the sampling period (which is typically constant – extension to the case of a time-varying sampling period is the subject of other research work). To facilitate the closed-loop stability analysis, we will also consider in the remainder of the paper that the operator \mathcal{Q}_s is invertible (or pseudo-invertible in the case of a non-square system). This requirement, which can be satisfied by appropriate selection of the locations of the measurement sensors [14], renders resetting the model output to match \bar{y} equivalent to resetting the model state to match \bar{x}_s , since $\omega(t_j) = \mathcal{Q}_s^{-1} \bar{y}(t_j)$.

B. Characterizing the minimum allowable sampling rate: A condition for ultimate boundedness

Defining the model estimation error $\bar{e}_s(t) = \omega(t) - \bar{x}_s(t)$, the augmented state $\xi = [\bar{x}_s \ \eta \ \bar{e}_s]^T$ in the extended state space $\mathcal{H}_s^\xi = \mathcal{H}_s \times \mathcal{H}_s \times \mathcal{H}_s$, the fault-free augmented slow system can be formulated as a combined discrete-continuous system and written in the following operator-matrix form:

$$\begin{aligned} \dot{\xi}(t) &= \Lambda^k \xi(t) + \mathcal{D} \theta(t), \quad t \in [t_j, t_{j+1}) \\ \bar{e}_s(t_j) &= 0, \quad j \in \{0, 1, 2, \dots\} \end{aligned} \quad (12)$$

where

$$\Lambda^k = \begin{bmatrix} \mathcal{A}_s & \mathcal{B}_s^k \mathcal{F}^k & \mathcal{O} \\ \mathcal{L} \mathcal{Q}_s & \mathcal{C} & \mathcal{L} \mathcal{Q}_s \\ \widehat{\mathcal{A}}_s & \widehat{\mathcal{B}}_s^k \mathcal{F}^k & \widehat{\mathcal{A}}_s \end{bmatrix}, \quad \mathcal{D} = \begin{bmatrix} \mathcal{W}_s \\ \mathcal{O} \\ -\mathcal{W}_s \end{bmatrix}, \quad (13)$$

$\mathcal{C} = \widehat{\mathcal{A}}_s + \widehat{\mathcal{B}}_s^k \mathcal{F}^k - \mathcal{L} \mathcal{Q}_s$ and $\widehat{\mathcal{A}}_s = \widehat{\mathcal{A}}_s - \mathcal{A}_s$, $\widehat{\mathcal{B}}_s^k = \widehat{\mathcal{B}}_s^k - \mathcal{B}_s^k$ represent the modeling errors. In order to derive conditions for closed-loop stability in terms of the sampling period, we need to express the closed-loop response as a function of the sampling period. The following proposition provides an explicit characterization of the sampled-data closed-loop system behavior in the absence of faults. The proof can be obtained by solving the linear system of (12)-(13) and using induction, and is omitted for brevity.

Proposition 1: The system described by (12) with initial condition $\xi(0) = [\bar{x}_s(0) \ \eta(0) \ \bar{e}_s(0)] = \xi_0$, has the following response:

$$\begin{aligned} \xi(t) &= \mathcal{T}_{\Lambda^k}(t - t_j) (\mathcal{N}_k)^j \xi_0 + \int_{t_j}^t \mathcal{T}_{\Lambda^k}(t - \tau) \mathcal{D} \theta(\tau) d\tau \\ &+ \mathcal{T}_{\Lambda^k}(t - t_j) \sum_{i=0}^{j-1} (\mathcal{N}_k)^i \mathcal{I}_o \Gamma_{j-i}, \quad t \in [t_j, t_{j+1}) \end{aligned} \quad (14)$$

where $\mathcal{T}_{\Lambda^k}(t) : \mathcal{H}_s^\xi \rightarrow \mathcal{H}_s^\xi$ is a C_0 -semigroup generated by Λ_k on \mathcal{H}_s^ξ , $\mathcal{N}_k = \mathcal{I}_o \mathcal{T}_{\Lambda^k}(\Delta) \mathcal{I}_o$, $\mathcal{I}_o = \text{diag}\{\mathcal{I} \ \mathcal{I} \ \mathcal{O}\}$, \mathcal{I} is the identity operator, and

$$\Gamma_j = \int_0^\Delta \mathcal{T}_{\Lambda^k}(\tau) \mathcal{D} \theta(t_j - \tau) d\tau, \quad j \in \{0, 1, 2, \dots\}$$

where $\Delta = t_{j+1} - t_j$.

Based on the result of Proposition 1, a necessary and sufficient condition for practical stability and ultimate boundedness of the state of the finite-dimensional closed-loop system under the sampled-data control structure can be obtained, and is presented in the following proposition.

Proposition 2: Consider the augmented system of (12)-(13), for a fixed $k \in \mathcal{K}$, with the initial condition $\xi(0) = \xi_0$, and let θ_b be a positive real number such that $|\theta(t)| \leq \theta_b$ for all $t \geq 0$. Then the state of the sampled-data closed-loop system is ultimately bounded if and only if $r(\mathcal{N}_k(\Delta)) < 1$.

Proof: Sufficiency can be shown by evaluating the norm of the solution given in (14), which yields, for $t \in [t_j, t_{j+1})$, $j \in \{0, 1, 2, \dots\}$:

$$\begin{aligned} \|\xi(t)\| &\leq \|\mathcal{T}_{\Lambda^k}(t - t_j) (\mathcal{N}_k)^j \xi_0\| + \left\| \int_{t_j}^t \mathcal{T}_{\Lambda^k}(t - \tau) \mathcal{D} \theta(\tau) d\tau \right\| \\ &+ \|\mathcal{T}_{\Lambda^k}(t - t_j) \sum_{i=0}^{j-1} (\mathcal{N}_k)^i \mathcal{I}_o \Gamma_{j-i}\| \end{aligned} \quad (15)$$

Since $r(\mathcal{N}_k) < 1$, we have $\|(\mathcal{N}_k)^j\| \leq \beta_k e^{-\gamma_k j}$, for some $\beta_k, \gamma_k > 0$, then the first term on the right hand side of (15) satisfies the following exponentially-decaying bound:

$$\|\mathcal{T}_{\Lambda^k}(t - t_j) (\mathcal{N}_k)^j \xi_0\| \leq \bar{\alpha}_k \bar{\beta}_k e^{-\bar{\gamma}_k t} \|\xi_0\| \quad (16)$$

where $\bar{\alpha}_k = e^{\mu_k \Delta}$, $\mu_k = \sup\{\text{Re } \sigma(\Lambda^k)\}$, $\bar{\beta}_k = \beta_k e^{\gamma_k}$ and $\bar{\gamma}_k = \gamma_k / \Delta > 0$. Evaluating the second term on the right hand side of (15) and using the fact that $\|\mathcal{T}_{\Lambda^k}(t)\| \leq e^{\mu_k t}$, one can obtain:

$$\begin{aligned} \left\| \int_{t_j}^t \mathcal{T}_{\Lambda^k}(t - \tau) \mathcal{D} \theta(\tau) d\tau \right\| &\leq \int_{t_j}^t e^{\mu_k(t-\tau)} \|\mathcal{D}\| \theta_b d\tau \\ &\leq \frac{\bar{\alpha}_k - 1}{\mu_k} \|\mathcal{D}\| \theta_b := F \end{aligned} \quad (17)$$

With (17) in mind, $\|\Gamma_{j-i}\|$ can also be bounded as follows:

$$\begin{aligned} \|\Gamma_{j-i}\| &\leq \int_0^\Delta e^{\mu_k \tau} \|\mathcal{D}\| \|\theta_b\| d\tau \\ &\leq \frac{e^{\mu_k \Delta} - 1}{\mu_k} \|\mathcal{D}\| \|\theta_b\| = \frac{\bar{\alpha}_k - 1}{\mu_k} \|\mathcal{D}\| \|\theta_b\| = F \end{aligned} \quad (18)$$

Substituting (18) into the third term on the right hand side of (15) and considering the fact that $\|\mathcal{I}_s\| = 1$, $\|\mathcal{T}_{\Lambda^k}(t-t_j)\| \leq \bar{\alpha}_k$ and $\|(\mathcal{N}_k)^i\| \leq \beta_k e^{-\gamma_k i}$, we have:

$$\begin{aligned} \|\mathcal{T}_{\Lambda^k}(t-t_j) \sum_{i=0}^{j-1} (\mathcal{N}_k)^i \mathcal{I}_s \Gamma_{j-i}\| &\leq \bar{\alpha}_k F \sum_{i=0}^{j-1} \beta_k e^{-\gamma_k i} \\ &\leq \frac{\bar{\alpha}_k \beta_k F}{1 - e^{-\gamma_k}} \end{aligned} \quad (19)$$

where we have used the fact that for $\gamma_k > 0$, $0 < e^{-\gamma_k} < 1$ and $0 < 1 - (e^{-\gamma_k})^j < 1$. Combining (16), (17) and (19), we conclude that:

$$\|\xi(t)\| \leq \bar{\alpha}_k \bar{\beta}_k e^{-\hat{\gamma}_k t} \|\xi_0\| + \delta_k(\Delta) \quad (20)$$

where $\delta_k(\Delta) := \frac{\bar{\alpha}_k \beta_k F}{1 - e^{-\gamma_k}} + F$, and consequently $\limsup_{t \rightarrow \infty} \|\xi(t)\| \leq \delta_k(\Delta)$, which implies that the state of the sampled-data closed-loop system is ultimately bounded if $r(\mathcal{N}_k(\Delta)) < 1$. To prove necessity, we proceed by contradiction. Let the state of the system of (12) be bounded and assume that \mathcal{N}_k has at least one eigenvalue outside the unit circle. This assumption implies that the first term on the right hand side of (14) will grow unbounded as time goes on, and therefore the third term cannot be bounded as well. Thus, we have a contradiction. This completes the proof. ■

Remark 1: It can be seen from the result of Proposition 2 and the structure of Λ_k in (13), that the spectral radius condition given in the proposition can be used to quantitatively examine the interplays between the maximum allowable sampling period, the choice of the inter-sample model predictor, the maximum disturbance size, and the choice of control actuator and measurement sensor locations. For example, for a fixed model, a given disturbance size, and given actuator/sensor locations, one can compute the maximum allowable sampling period that ensures bounded stability. Alternatively, for a fixed sampling period, one can use the stability condition to determine the maximum allowable disturbance size, the maximum allowable plant-model mismatch, as well as the range of allowable actuator/sensor locations that ensure bounded stability. Note also from the proof of Proposition 2 that the ultimate bound is dependent on all these parameters and can be tuned by appropriate selection of the sampling period, the model and the actuator/sensor locations. Finally, since \mathcal{N}_k is defined over a finite-dimensional space, its spectral radius can be determined by computing the eigenvalues of \mathcal{N}_k .

IV. ROBUST FINITE-DIMENSIONAL FAULT-TOLERANT CONTROL SYSTEM DESIGN

A. Fault detection using a time-varying alarm threshold

To determine the fault or health status of the control actuators in the operating control configuration, the state observer in (10) is used as a fault detection filter and its output is compared with the actual output at the sampling times. The following proposition provides an explicit characterization of

the expected fault-free evolution of the residual, which can be used as the basis for fault detection.

Proposition 3: Consider the closed-loop system of (9) and (11), for a fixed control configuration, $k \in \mathcal{K}$, with $f_a^k \equiv 0$, and consider the augmented system of (12)-(13) where the sampling period Δ is chosen such that $r(\mathcal{N}_k(\Delta)) < 1$. Then there exist positive real numbers, $\hat{\alpha}_k > 1$, $\hat{\beta}_k$, and a continuous function, $\hat{\delta}_k(\cdot)$, such that the residual defined by $r_d(t) = \|\bar{y}(t) - \mathcal{Q}_s \eta(t)\|$ satisfies a time-varying bound:

$$r_d(t) \leq \hat{\alpha}_k \|\xi_0\| e^{-\hat{\gamma}_k t} + \hat{\delta}_k(\Delta, \theta_b), \quad \forall t \geq 0 \quad (21)$$

Proof: Since $\bar{y} = \mathcal{Q}_s \bar{x}_s$ and the operator \mathcal{Q}_s is bounded, we have $r_d(t) \leq \|\mathcal{Q}_s\| \|\bar{x}_s(t) - \eta(t)\| \leq k_1 \|\bar{x}_s(t) - \eta(t)\|$, for some $k_1 > 0$. From the result of Proposition 2, we have that if Δ is chosen such that $r(\mathcal{N}_k(\Delta)) < 1$, then (20) is satisfied. This, together with the facts that $\|\bar{x}_s(t)\| \leq \|\xi(t)\|$ and $\|\eta(t)\| \leq \|\xi(t)\|$, implies that $r_d(t) \leq 2k_1 \|\xi(t)\| \leq 2k_1 \bar{\alpha}_k \bar{\beta}_k e^{-\hat{\gamma}_k t} \|\xi_0\| + 2k_1 \delta_k(\Delta, \theta_b)$. Finally, the bound in (21) can be established by identifying $\hat{\alpha}_k = 2k_1 \bar{\alpha}_k \bar{\beta}_k$, $\hat{\gamma}_k = \hat{\gamma}_k$, and $\hat{\delta}_k(\Delta, \theta_b) = 2k_1 \delta_k(\Delta, \theta_b)$. ■

Remark 2: The result of Proposition 3 suggests that, for a given sampling rate that satisfies the stability condition and a given upper bound on the disturbance size, a fault can be declared at time T_d if the residual breaches the time-varying alarm threshold given in (21), i.e.,:

$$r_d(T_d) > \hat{\alpha}_k \|\xi_0\| e^{-\hat{\gamma}_k T_d} + \hat{\delta}_k(\Delta) \implies f_a^k(T_d) \neq 0 \quad (22)$$

Note that the alarm threshold accounts for the influences of sampling and external disturbances. Note also that the residual can be evaluated only at the sampling times, i.e., fault detection can take place only at t_j , $j \in \{0, 1, 2, \dots\}$ regardless of when the fault actually occurs. In general, detection delays can be minimized by proper choice of the constants $\hat{\alpha}_k$ and $\hat{\gamma}_k$ to ensure that the threshold is sufficiently tight, however, the smallest possible delay is ultimately determined by the given sampling rate.

B. Stability-based control actuator reconfiguration

Following the detection of a fault in the operating actuator configuration, corrective action in the form of switching to a healthy fall-back actuator configuration is needed to preserve robust closed-loop stability. Given the dependence of the actuator configuration (i.e., the spatial placement of the control actuators) on the measurement sampling rate (see Proposition 2 and Remark 1), the fall-back actuators must be chosen such that the given sampling rate continues to be stabilizing in the absence of faults. This logic is formalized in Theorem 1 below. The proof follows directly from the result of Proposition 2 and is omitted for brevity.

Theorem 1: Consider the closed-loop system of (9) and (11), where $|\theta(t)| \leq \theta_b$, for some $\theta_b > 0$, for some $i \in \mathcal{K}$, and the sampling period Δ is chosen such that $r(\mathcal{N}_i(\Delta)) < 1$. Let T_f be the earliest time such that a fault is detected. Then the following switching rule:

$$k(t) = \begin{cases} i, & 0 \leq t < T_f \\ \nu \neq i, & t \geq T_f, r(\mathcal{N}_\nu(\Delta)) < 1 \end{cases} \quad (23)$$

guarantees that the state of the switched closed-loop system is ultimately bounded.

Remark 3: In cases where several actuator configurations satisfy the stability requirement, it is possible to incorporate

additional performance criteria in the switching logic to narrow down the number of possible candidates. For example, one can select the configuration that enforces the smallest ultimate bound. Note also that while Theorem 1 considers the case of a single fault, the same logic can be applied in cases of multiple consecutive faults. In this case, however, and given the fact that the structure of Λ^k changes after each actuator switching, a new alarm threshold should be used for the residual following each actuator switching to allow for the detection of future faults.

Remark 4: It can be shown that the robust fault-tolerant control system designed on the basis of the approximate finite-dimensional system continuous to enforce fault-tolerance in the infinite-dimensional system provided that the separation between the slow and fast eigenvalues of the differential operator is sufficiently large. This argument can be justified using singular perturbation techniques (e.g., [21], [22]) and is omitted for brevity.

V. SIMULATION STUDY

In this section, we illustrate through computer simulations how the robust fault detection and fault-tolerant control methodology earlier can be used to robustly stabilize the open-loop unstable zero solution of a linearized diffusion-reaction process of (1) subject to the boundary and initial condition of (2), where $\alpha = 1$, $\beta = 1.66$ and $\omega = \nu = 2$. It can be verified that the operating steady state $\bar{x}(z, t) = 0$ (with $u = \theta = f_a = 0$) is unstable. Therefore the control objective is to stabilize the closed-loop system near this unstable steady state in presence of external disturbance and actuator faults. We consider the first eigenvalue as the dominant one and use standard Galerkins method to derive an ODE that describes the temporal evolution of the amplitude of the first eigenmode of the fault-free system: $\dot{a}_1 = \lambda_1 a_1 + g(z_a)u + \omega(z_d)\theta$, where $\bar{x}(z, t) = \sum_{i=1}^{\infty} a_i(t)\phi_i(z)$, $g(z_a) = \beta_U \langle \phi_1(z), b(z) \rangle$, $\omega(z_d) = \beta_U \langle \phi_1(z), d(z) \rangle$, and a single point actuator (with finite support) is used for stabilization, i.e., $b(z) = 1/(2\mu)$ for $z \in [z_a - \mu, z_a + \mu]$, where μ is a sufficiently small number, and $b(z_a) = 0$ elsewhere. This ODE is used to design the output feedback controller and fault detection filters which are then implemented on a 30th order Galerkin discretization of the PDE (higher order discretizations led to identical results).

Following the methodology outlined in Section IV, we consider a feedback controller of the form: $u = F^k \eta$, where F^k is the feedback gain, η is an estimate of a_1 generated by an observer: $\dot{\eta} = \hat{\lambda}_1 \eta + \hat{g}(z_a)u + L(y - Q_s(z_s)\eta)$, $y(t) = \langle q(z), \bar{x}(z, t) \rangle$, provided by a point sensor located at z_s where $Q_s(z_s) = \langle q(z), \phi_1(z) \rangle$, $q(z)$ is sensor distribution function. Following the analysis presented in Section III, it can be verified that the closed-loop system is ultimately bounded if and only if the spectral radius of the matrix $N_k = I_0 e^{\Lambda^k \Delta} I_0$ is less than one, where:

$$\Lambda^k = \begin{bmatrix} \lambda_1 & g(z_a^k)F^k & 0 \\ LQ_s(z_s) & \hat{\lambda}_1 + \hat{g}(z_a^k)F^k - LQ_s(z_s) & LQ_s(z_s) \\ \hat{\lambda}_1 - \lambda_1 & [\hat{g}(z_a^k) - g(z_a^k)]F^k & \hat{\lambda}_1 \end{bmatrix}$$

and $I_0 = \text{diag}\{1 \ 1 \ 0\}$.

We consider the first case when no faults are present in the operating actuator configuration, and analyze the dependence of closed-loop stability on the selection of the actuator location and the sampling period where a point disturbance is introduced at $z_d = \pi/8$ with an amplitude $\theta_b = 0.2$. The contour plots in Fig.1 show the dependence of the spectral radius of N_k (plot(a)) and the size of the ultimate bound (plot(b)) on both the actuator location, z_a and the sampling period, Δ , when an uncertain model (with $\hat{\lambda}_1 = 0.3$ and $\hat{g}(z_a) = 0.5$) is used to estimate the evolution of a_1 between sampling instances and the output feedback controller is designed with $F = -15$ and $L = 100$, respectively. The uncolored area in Fig.1(a), which is enclosed by the unit contour lines, represents the stability region within which the sampled-data closed-loop system can be robustly stabilized under a given control configuration. It can be seen that the set of stabilizing actuator locations increases as the sampling period decreases, and that the maximum stabilizing sampling period shrinks as the actuator is moved closer to the middle. In Fig.1(b), the value of each contour line represents an upper bound on the size of the terminal set that the closed-loop state will converge to when the values of actuator location and sampling period are chosen within the stability region shown in Fig.1(a). As expected, for a given ultimate bound, the range of stabilizing actuator locations shrinks as the sampling period is increased. Also, for a given actuator placement, the size of the terminal set grows as the sampling period is increased (i.e., the performance deteriorates). The prediction of Fig.1 are confirmed in Fig.2 which shows that the closed-loop system is robustly stable around zero solution for $(\Delta = 0.2, z_a = 0.25)$ (a) and becomes unstable for $(\Delta = 0.2, z_a = 1.5)$ (b).

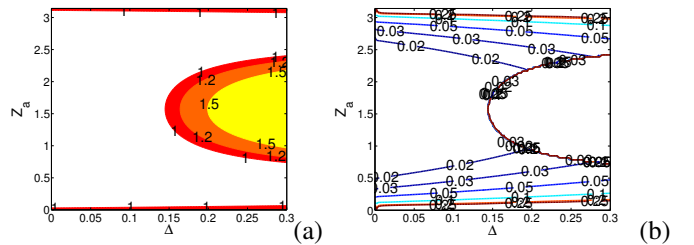


Fig. 1. Dependence of the spectral radius of N_k (a) and the ultimate bound (b) on the sampling period and actuator location, for a fixed model predictor

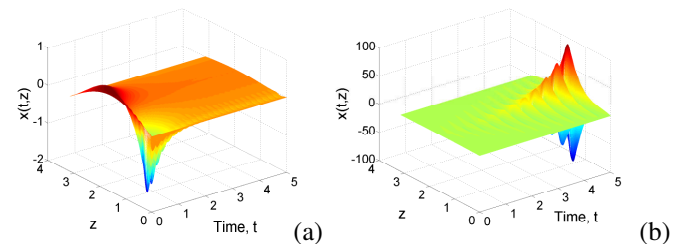


Fig. 2. Closed-loop state profiles for $(\Delta = 0.2, z_a = 0.25)$ (a) and $(\Delta = 0.2, z_a = 1.5)$ (b) in the presence of external disturbances, and in the absence of faults

To illustrate the fault detection and handling capabilities of the sampled-data control system, the process is initialized using a healthy actuator placed at $z_a = 0.25$ with the sampling period $\Delta = 0.2$. Based on the evolution of the

residual in the absence of faults, a time-varying bound of the form: $r_d(t) = 0.4e^{-0.05t} + 0.005$ is used as an alarm threshold for fault detection. In order to ensure fault-tolerance, two backup control actuators, placed at $z_a = 0.6$ and $z_a = 1.5$, respectively. At $T_f = 2.0$, a fault is introduced in the operating actuator. As can be seen from Fig. 4(a), the fault is detected at $T_d = 2.2$ when it causes the residual to breach the alarm threshold. At this time, the supervisor needs to switch to a backup actuator to maintain closed-loop stability. For the given sampling period, it can be seen from Fig.1(a) that the actuator placed at $z_a = 0.6$ lies inside the unit contour line and is therefore expected to be stabilizing, while the actuator placed at $z_a = 1.5$ lies outside and therefore can not stabilize the closed-loop system. This prediction is confirmed by the closed-loop state profiles in panels (a) and (b) in Fig.3. It can also be seen in Fig.4(a) that following the activation of the new actuator, a new residual threshold is calculated and used so as to allow for continued fault detection in the new configuration (see the red profiles).

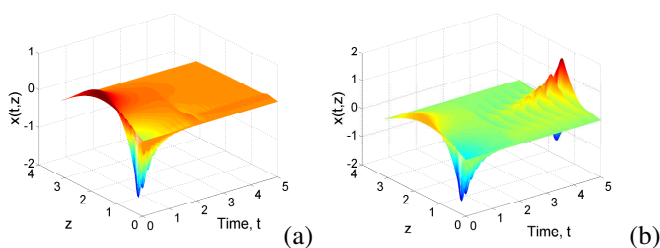


Fig. 3. Closed-loop state profiles when a fault is detected in the primary actuator and subsequent reconfiguration to an actuator placed at $z_a = 0.6$ (a) and to an actuator at $z_a = 1.5$ (b) take place

In addition to closed-loop stability considerations, we have also investigated the performance-based reconfiguration to determine the best actuator configuration which the control system switch to when all the backup candidates can successfully stabilize the closed-loop system. In this case, we choose two point actuator at $z_a = 0.6$ and $z_a = 0.15$, respectively. From Fig.1(a), it can be seen that while both backup actuators lie inside the unit contour zone (for $\Delta = 0.2$), Fig.1(b) shows that the actuator placed at $z_a = 0.6$ enforces a smaller ultimate bound than the one located at $z_a = 0.15$. This is confirmed in Fig.4(b), which shows that following fault detection at $T_d = 2.2$, the amplitude of the first eigenmode settles closer to zero when the actuator located at $z_a = 0.6$ is activated (black), while the steady state offset is larger when the actuator at $z_a = 0.15$ is activated (red).

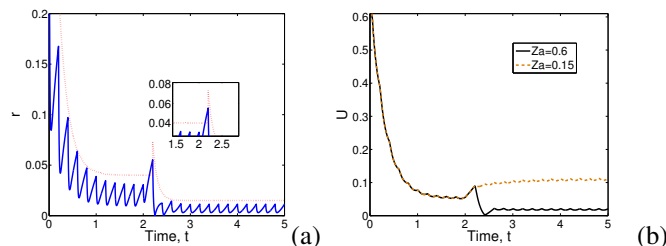


Fig. 4. (a): Evolution of the residual (blue) when a fault is introduced at $T_f = 2.0$ in the primary actuator and subsequent reconfiguration to an actuator placed at $z_a = 0.6$ takes place. b(b): Evolution of the first eigenmode when the actuator placed at $z_a = 0.6$ (black) or at $z_a = 0.15$ (red) is activated, respectively, following fault detection.

REFERENCES

- [1] D. M. Himmelblau, *Fault Detection and Diagnosis in Chemical and Petrochemical Processes*. New York: Elsevier Scientific Pub., 1978.
- [2] P. M. Frank and X. Ding, "Survey of robust residual generation and evaluation methods in observer-based fault detection systems," *J. Proc. Contr.*, vol. 7, pp. 403–424, 1997.
- [3] C. DePersis and A. Isidori, "A geometric approach to nonlinear fault detection and isolation," *IEEE Trans. Automat. Contr.*, vol. 46, pp. 853–865, 2001.
- [4] S. Simani, C. Fantuzzi, and R. Patton, *Model-based Fault Diagnosis in Dynamic Systems Using Identification Techniques*. London: Springer, 2003.
- [5] M. Blanke, M. Kinnaert, J. Lunze, and M. Staroswiecki, *Diagnosis and Fault-Tolerant Control*. Berlin-Heidelberg: Springer, 2003.
- [6] L. Cheng, E. Kwok, and B. Huang, "Closed-loop fault detection using local approach," *Can. J. Chem. Eng.*, vol. 81, pp. 1101–1108, 2003.
- [7] V. Venkatasubramanian, R. Rengaswamy, K. Yin, and S. N. Kavuri, "Review of process fault diagnosis - parts I, II, III," *Comp. & Chem. Eng.*, vol. 27, pp. 293–346, 2003.
- [8] X. D. Zhang, T. Parisini, and M. M. Polycarpou, "Adaptive fault-tolerant control of nonlinear uncertain systems: An information-based diagnostic approach," *IEEE Trans. Automat. Contr.*, vol. 49, pp. 1259–1274, 2004.
- [9] B. Huang, "Bayesian methods for control loop monitoring and diagnosis," *J. Proc. Contr.*, vol. 18, pp. 829–838, 2008.
- [10] P. Mhaskar, C. McFall, A. Gani, P. D. Christofides, and J. F. Davis, "Isolation and handling of actuator faults in nonlinear systems," *Automatica*, vol. 44, pp. 53–62, 2008.
- [11] S. Perk, F. Teymour, and A. Cinar, "Statistical monitoring of complex chemical processes using agent-based systems," *Ind. & Eng. Chem. Res.*, vol. 49, pp. 5080–5093, 2010.
- [12] W. H. Ray, "Some recent applications of distributed parameter systems theory - a survey," *Automatica*, vol. 14, pp. 281–287, 1978.
- [13] P. D. Christofides and P. Daoutidis, "Finite-dimensional control of parabolic PDE systems using approximate inertial manifolds," *J. Math. Anal. Appl.*, vol. 216, pp. 398–420, 1997.
- [14] P. D. Christofides, *Nonlinear and Robust Control of PDE Systems: Methods and Applications to Transport-Reaction Processes*. Boston: Birkhäuser, 2001.
- [15] D. Del Vecchio and N. Petit, "Boundary control for an industrial under-actuated tubular chemical reactor," *J. Proc. Contr.*, vol. 15, pp. 771–784, 2005.
- [16] S. Dubljevic, "Model predictive control of kuramoto-sivashinsky equation with state and input constraints," *Chem. Eng. Sci.*, vol. 65, pp. 4388–4396, 2010.
- [17] A. Smyshlyaev and M. Krstic, *Adaptive Control of Parabolic PDEs*. Princeton University Press, 2010.
- [18] H. Baruh, "Actuator failure detection in the control of distributed systems," *Journal of Guidance, Control, and Dynamics*, vol. 9, pp. 181–189, 1986.
- [19] M. Demetriou, K. Ito, and R. Smith, "Adaptive monitoring and accommodation of nonlinear actuator faults in positive real infinite dimensional systems," *IEEE Trans. Automat. Contr.*, vol. 52, pp. 2332–2338, 2007.
- [20] A. Armaou and M. Demetriou, "Robust detection and accommodation of incipient component faults in nonlinear distributed processes," *AIChE J.*, vol. 54, pp. 2651–2662, 2008.
- [21] N. H. El-Farra and S. Ghantasala, "Actuator fault isolation and reconfiguration in transport-reaction processes," *AIChE J.*, vol. 53, pp. 1518–1537, 2007.
- [22] S. Ghantasala and N. H. El-Farra, "Robust actuator fault isolation and management in constrained uncertain parabolic PDE systems," *Automatica*, vol. 45, pp. 2368–2373, 2009.
- [23] M. Mahmood and P. Mhaskar, "Safe-parking framework for fault-tolerant control of transport-reaction processes," *Ind. & Eng. Chem. Res.*, vol. 49, pp. 4285–4296, 2010.
- [24] S. Ghantasala and N. H. El-Farra, "Actuator fault detection and reconfiguration in distributed processes with measurement sampling constraints," in *Proceedings of American Control Conference*, St. Louis, MO, 2009, pp. 1523–1529.
- [25] R. F. Curtain and A. J. Pritchard, *Infinite Dimensional Linear Systems Theory*. Berlin-Heidelberg: Springer-Verlag, 1978.